IEEE Access
Multidisciplinary | Rapid Review | Open Access Journal

Received September 4, 2020, accepted October 12, 2020, date of publication October 28, 2020,
date of current version December 2, 2020.

*Digital Object Identifier 10.1109/ACCESS.2020.3034326*

# Research on Shaking Table Test of Earthquake Simulation Based on Hybrid Integration Algorithm

**YING-QING GUO[1,2], ZONG-YIN LI[1], XIAO-LU YANG[1], AND JIN-BAO LI[3]**
[1]College of Mechanical and Electronic Engineering, Nanjing Forestry University, Nanjing 210037, China
[2]Nanjing Dongrui Damping Control Technology Company Ltd., Nanjing 210033, China
[3]Jiangsu Southeast Special Engineering and Technology Company Ltd., Nanjing 210008, China

Corresponding author: Ying-Qing Guo (gyingqing@njfu.edu.cn)

This work was supported in part by the National Natural Science Foundation of China under Grant 51878355 and in part by the National Key R&D Programs of China under Grant 2019YFE0121900.

**ABSTRACT** Aiming at the problem of poor accuracy of acceleration waveform reproduction during the shaking table test of earthquake simulation, a hybrid integration algorithm based on seismic acceleration signal is proposed to control the trend term error. The low-frequency attenuation integral algorithm in the frequency domain is used to integrate the original seismic acceleration signal once to obtain the vibration velocity signal, then, the polynomial fitting integration algorithm is introduced to integrate of the vibration velocity signal once in the time domain to obtain the vibration displacement signal. Through these two integrals, the sensitivity of low frequency band during frequency domain integration and the accumulation of small errors in time domain are reduced. Finally, the hybrid integration algorithm is used to perform seismic wave reproduction experiments on the seismic simulation shaker and good results are obtained, which proves that the hybrid integration calculation has high practical value and practical significance in improving the accuracy of the vibration table waveform reproduction.

**INDEX TERMS** Earthquake simulation shaker, hybrid integration algorithm, low frequency attenuation, polynomial fitting, seismic wave reproduction.

## I. INTRODUCTION

Earthquake simulation shaking table is a research material or building structure under earthquake or specific vibration that can more realistically simulate the state of stress and failure form of the structure under the action of seismic load. It is one of the commonly used test methods in the field of structural seismic research and over-limit design [1], [2], and has been widely used in the field of bridge engineering, civil engineering and Marine structural engineering [3]. However, on the one hand, due to the difference between the seismic simulation test and other vibration tests, the earthquake mainly generates infra-sound waves, and the energy of the seismic waves is mainly concentrated in the low frequency band the earthquake generated mainly is infra-sound, and the energy of the seismic wave is mainly concentrated in the low frequency band. In addition, the lower limit frequency of the seismic wave signal is relatively low, so the low-frequency performance of the seismic simulation shaking table is highly required [4]. On the other hand, in the real vibration occurrence site, the detection of the signal displacement response is very troublesome, and even for some reasons, it cannot be directly measured, so most natural signals such as seismic waves are stored in the form of acceleration, at present, the displacement and velocity time-history curves of the test waveform need to be obtained in most seismic simulation shaking table tests, and the control signal required for each action of the servo motor is calculated through these two curves. Therefore, the integration processing of the acceleration signal has become an indispensable part in the shaking table test.

At present, the most commonly used integration algorithms are mainly divided into frequency domain integration and time domain integration [5]. The low-frequency cut-off integral algorithm is the most common one in the frequency domain integral algorithm [6], [7], which sets a low-frequency cut-off frequency on the basis of the Fourier transform and zeros the signals below this frequency, although this method can effectively avoid the influence of the trend term on the integration result, it also causes the loss

The associate editor coordinating the review of this manuscript and approving it for publication was Hongwei Du.

of some effective signals. Gu and Lv [8] proposed that the low-frequency amplitude in the amplitude spectrum after the vibration acceleration undergoes FFT transformation should be set to zero, and then the vibration displacement signal could be obtained after IFFT transform in two integrations in the frequency domain. Hu *et al.* [9] used a low-frequency attenuation algorithm to directly integrate the acceleration signal within the frequency, and used the integration accuracy control equation to ensure the integration accuracy. Within the scope of the time domain integration algorithm, it is more common to process the data by adding various filters. Wang and Wang [10] used the moving window method to intercept three signal values to establish a Lagrange quadratic polynomial, and integrated the polynomial at the same time, thereby deriving an easy-to-program calculation formula to perform the integral operation. In addition, several studies have been explored to improve the integration error and accuracy, such as energy-consistent time integration [11] and integration algorithm optimization [12], [13]. Zhang and Zheng [14] developed an integration algorithm based on Walsh transformation and empirical mode decomposition (EMD), and removed the trend terms of velocity and displacement through linear least squares fitting. Zhu *et al.* [15] provided a novel vibration signal integral method based on feature information extraction to deal with nonlinear and non-stationary signals, this research merged the superposition of kurtosis, mean square error, energy, and singular value decomposition on signal feature extraction. Comparing with the traditional integral methods, this method shows higher accuracy and superiority.

In order to better control the cumulative error of the second integral of the speed signal in the seismic simulation shaking table test, based on the characteristics of time domain integration and frequency domain integration, a hybrid integral algorithm is designed to improve the integral error of shaking table test. First, the low-frequency attenuation integration algorithm in the frequency domain is used to integrate the original seismic acceleration signal once to obtain the vibration velocity signal, which is mainly used to control the low-frequency trend term error. Then, a polynomial fitting integration algorithm is used to integrate the vibration velocity signal again in the time domain, and the residual small errors in the integration are fitted, so as to obtain the final vibration displacement signal. The research shows that the hybrid integration algorithm can effectively improve the integration error compared to other single time-domain or frequency-domain integration, and the engineering application characteristics of the algorithm are summarized through seismic wave simulation shaking table tests. The research results of this paper have certain reference value for the follow-up integral error control research and engineering application.

## II. PRINCIPLE OF INTEGRAL ALGORITHM

### A. TIME DOMAIN INTEGRATION ALGORITHM

The numerical integral of the trapezoidal integral is usually adopted, in which the initial displacement and initial velocity of the original acceleration signal are added to the calculation. At the same time, the integration result is usually accompanied by a very obvious trend term, the zero drift phenomenon. Therefore, the collected original seismic wave acceleration signal contains not only a DC component, but also an error term that changes with time [16], if $a_n(t)$ is the acceleration corresponding to the seismic wave measured at time $t$, then $a_n(t)$ can be expressed as:

$$a_n(t) = a_0(t) + a_e(t) = a_0(t) + a_m(t) + D \tag{1}$$

where: $a_0(t)$ is the true acceleration; $a_e(t)$ is the measured acceleration error; $a_m(t)$ is the error that changes with time; $D$ is the DC component of the measured acceleration signal.

Trapezoidal formula is used to numerically integrate $a_n(t)$, where there is an error $e(t)$ in the process of integrating velocity $v(t)$ to obtain displacement $s(t)$. The expression in the two integration process can be expressed as:

$$v(t) = \int a_n(t)dt = \int a_0(t)dt + \int a_m(t)dt + Dt + C \tag{2}$$

$$e(t) = \int v(t)dt - \int \left( \int a_0(t)dt \right) dt \tag{3}$$

$$s(t) = \int \left( \int a_n(t)dt \right) dt - \int \left( \int a_m(t)dt \right) dt - 0.5Dt^2 - Ct - F \tag{4}$$

where: $C$ is the constant error of speed; $F$ is the constant error of displacement.

When the time-varying error $a_m(t)$ is a linear term, the corresponding displacement $s(t)$ is obtained by fitting $e(t)$ with polynomials; when the integral trend term generated by $a_m(t)$ is generated by random noise in the signal, a high-pass filter needs to be added [17], [18] to eliminate the error $e(t)$ to obtain the displacement in Eq. (4), this can improve the integration accuracy of the displacement obtained by the final integration

### B. FREQUENCY DOMAIN INTERGRATION ALGORITHM

Any continuously measured sequence or signal can calculate the frequency, phase, and amplitude of different sine wave signals by accumulating the original signal on the basis of Fourier transform. Then the sinusoidal signals of different frequencies are infinitely superimposed to represent the corresponding signals or sequences [19], [20]. Therefore, the acceleration signal $a_n(t)$ with the number of sampling points $N$ can be dispersed into the acceleration sequence $\{a_n\}$, and then transformed into a complex sequence $\{a_k\}$ in the frequency domain by FFT, and the formula for performing two frequency domain integration in the spectrum is:

$$A(k) = \sum_{n}^{N} a_n e^{-j(2\pi nk/N)} \tag{5}$$

$$V(k) = \frac{A(k)}{jwk} = \sum_{n=1}^{N} \frac{1}{2\pi kj\Delta f} H(k) a_n e^{-2\pi njk/N} \tag{6}$$

$$S(k) = \frac{A(k)}{-w^2 k} = \sum_{n=1}^{N} \frac{1}{(2\pi kj\Delta f)^2} H(k) a_n e^{-2\pi njk/N} \quad (7)$$

where: $A(k)$ is the acceleration spectrum; $N$ is the number of integration sampling points; $v(k)$ represents the velocity spectrum; $s(k)$ represents the displacement spectrum; $\Delta f$ spectral resolution; $n, K$ is a positive integer; $Wk$ is the frequency corresponding to the Fourier component. In particular, the following conditions are satisfied for $H(k)$ in Eq. (6) and Eq. (7):

$$H(k) = \begin{cases} 0 & fi \le k\Delta f \le f_H \\ 1 & \text{others} \end{cases} \quad (8)$$

where: $f_L$ is the lower cut-off frequency, and $f_H$ is the upper cut-off frequency.

The velocity $v(k)$ and displacement $S(k)$ generated in the frequency spectrum are transformed by IFFT to obtain the corresponding velocity $v(t)$ and displacement $S(t)$ in the time domain. Due to the existence of low-frequency signals, a larger frequency domain integration error will occur when $Wk$ is smaller, but compared to the time domain integration algorithm, the frequency domain integration algorithm has high operation efficiency, it can not only effectively avoid the complexity of removing the trend term for each integration in the time domain, but also avoid the energy loss caused by reducing the trend term. Based on the trend term in frequency domain integration mainly focuses on low frequency band, in order to effectively reduce the error caused by low frequency band signal, it can be considered to introduce low frequency function $g(wk)$ to control the integration process in frequency domain [21]. Among them, the most important thing about the low-frequency function $g(wk)$ is to select the appropriate cut-off frequency $f_T$ and integration accuracy $\alpha T$. However, the selection of the integration accuracy $\alpha T$ should be based on the low-frequency noise level of the signal, and the larger value should be selected as far as possible on the basis of controlling the trend error (it is recommended that 0.92 to 0.99).Thus, the effective information in the signal can be fully retained. At present, the main methods are low-frequency cut-off integral algorithm and low-frequency attenuation algorithm.

## III. PRINCIPLE OF MIXED INTEGRAL CALCULATION

Through the above analysis of the integration characteristics of the time domain and the frequency domain, it is found that the error generated by the second integration in the time domain is larger than the error generated by the first integration, and the second integral in the frequency domain is also greater than the first integral due to the influence of low-frequency characteristics [22]. Therefore, a hybrid integration algorithm is designed by comprehensively considering the main sources of errors in each link in the time-frequency integration process. First, the original seismic wave acceleration signal $a_n(t)$ is integrated with the low-frequency attenuation integration algorithm in the frequency domain and converted into a time-domain velocity signal $v(t)$. Then, in the time domain, a polynomial fitting integration algorithm is used to perform the integral operation on the obtained speed signal $v(t)$ again, and the linear error remaining in the integration is also fitted, thereby obtaining the final displacement signal $s(t)$. The flow chart of the hybrid integration algorithm is shown in Figure.1.

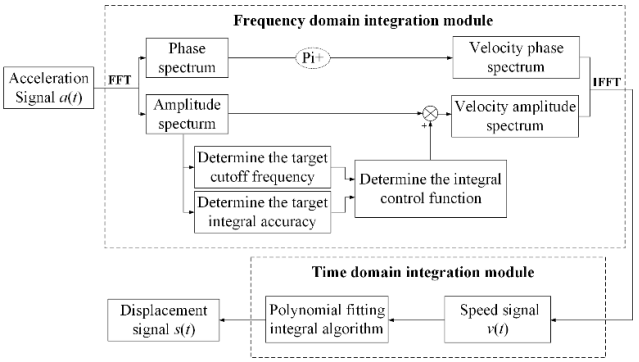


**FIGURE 1.** Flow chart of hybrid integration algorithm.

### A. FREQUENCY DOMAIN INTEGRATION MODULE

The principle of conversion between acceleration and displacement of low-frequency attenuation algorithm in the literature [23] is compared, and the least square method is used to control the integration error in the frequency domain. To this end, the goal of the integration trend term for the $a_n(t)$ input and $v(t)$ output during the integration process is established. The function equation is:

$$\underset{v}{Min}\ \Pi(v) = 0.5\beta^2 \int_{T_1}^{T_2} v^2 dt + 0.5 \int_{T_1}^{T_2} \left(\frac{dv}{dt} - an\right)^2 dt \quad (9)$$

where: $\beta$ is the regularization factor.

The former term in Eq. (9) controls the error of the trend term by introducing a regularization factor $\beta$, and the latter term is used to control the loyalty of the integration process to $a_n(t)$. The expansion formula after derivation of Eq. (9) is:

$$\begin{aligned} \delta\Pi(v) &= \beta^2 \int_{T_1}^{T_2} v\delta v dt + \int_{T_1}^{T_2} \frac{d\delta v}{dt}\left(\frac{dv}{dt} - a_n\right) dt \\ &= \int_{T_1}^{T_1} \delta v \left(\frac{d^2 v}{dt^2} + \beta^2 v - \frac{da_n}{dt}\right) dt \\ &\quad + \delta v \left(\frac{dv}{dt} - a_n\right)\Big|_{T}^{T_2} = 0 \end{aligned} \quad (10)$$

According to the Eq. (10), the establishment of the medium formula should satisfy the following relationship:

$$\begin{cases} \dfrac{d^2 v}{dt^2} + \beta^2 v = \dfrac{da_n}{dt} \\ \dfrac{dv}{dt} = a_n \end{cases} \quad (11)$$

Through the derivation and solution of Eq. (10) and Eq. (11), the frequency response function $H_B(f)$ transferred from the acceleration $a_n(t)$ to the velocity $v(t)$ during the

integration process can be obtained as:

$$H_B(f) = \frac{v(w_k)}{a_n(w_k)} = -\frac{w_k}{w^2k + \beta^2} \tag{12}$$

where: $H_B(f)$ is the frequency response function; $wk$ is the circular frequency.

Since the regularization factor $\beta$ can be represented by the set cut-off frequency $f_T$ and integration accuracy $\alpha T$, its low-frequency velocity integral control function $g_v(w_k)$ can be expressed as:

$$g_v(w_k) = \frac{w_k}{w^2k + \frac{1-\alpha T}{\alpha T}(2\pi f_T)^2} \tag{13}$$

where: $f_T$ is the cutoff frequency; $\alpha T$ is the integration accuracy, the value is 0.98.

According to the principle of frequency domain integration and the inverse Fourier transform law, its velocity signal $v(t)$ can be expressed as:

$$\begin{aligned} v(t) &= F^{-1}\left[\frac{1}{w_k} g_v(w_k) F[a_n(t)]\right] \\ &= F^{-1}\left[\frac{F[a_n(t)]}{w^2k + \frac{1-\alpha T}{\alpha T}(2\pi f_T)^2}\right] \end{aligned} \tag{14}$$

### B. TIME DOMAIN INTERGRATION MODULE

The speed signal $v(t)$ obtained on the basis of the frequency domain integration module is calculated by numerical integration using Simpson's law to obtain the displacement signal $s(t)$ as follows:

$$s(t) = s(t-1) + \frac{v(t-1) + 4v(t) + v(t+1)}{6} \times \Delta t \tag{15}$$

where: $t = 0, 1, \ldots N-1$; $\Delta t$ is the sampling time, and when $t - 1 \leq 0$, its value is 0.

The polynomial fitting integration algorithm is used to fit and remove the error $e(t)$ generated during the integration process. According to the time domain curve, the quadratic polynomial $y(t)$ is calculated and fitted by using Gauss to minimize the sum $I$ of squares of the difference between displacement $s(t)$ and $t(t)$. The calculation process is as follows:

$$I = \sum_{i=0}^{n-1}\left[S_i - x_2 t_t^2 - x_1 t_i - x_0\right]^2 \tag{16}$$

The partial derivative of Eq. (16) can be obtained:

$$\begin{cases} \dfrac{\partial I}{\partial x_2} = -2\displaystyle\sum_{i=0}^{n-1}\left[Si - x2t_i^2 - x_1 t_i - x_0\right] t_i^2 \\ \dfrac{\partial I}{\partial x_1} = -2\displaystyle\sum_{i=0}^{n-1}\left[Si - x_2 t_i^2 - x_i t_i - x_0\right] t_i \\ \dfrac{\partial I}{\partial x_0} = -2\displaystyle\sum_{i=0}^{n-1}\left[Si - x_2 t_i^2 - x_1 t_i - x_0\right] \end{cases} \tag{17}$$

where: $n$ is the number of discrete points, $x_2, x_1, x_0$ is the coefficient of $y(t)$.

In order to minimize the square sum $I$ of the difference between the displacements $s(t)$ and $y(t)$, the partial derivatives of $I$ in Eq. (17) are all 0.

$$\begin{cases} \displaystyle\sum_{i=0}^{n-1} t_i^2 s_t = x_2\sum_{i=0}^{n-1} t_i^4 + x_1\sum_{i=0}^{n-1} t_i^3 + x_0\sum_{i=0}^{n-1} t_i^2 \\ \displaystyle\sum_{i=0}^{n-1} t_{iSi} = x_2\sum_{i=0}^{n-1} t_i^3 + x_1\sum_{i=0}^{n-1} t_i^2 + x_0\sum_{i=0}^{n-1} t_i \\ \displaystyle\sum_{i=0}^{n-1} s_i = x_2\sum_{i=0}^{n-1} t_i^2 + x_1\sum_{i=0}^{n-1} t_i + nx_0 \end{cases} \tag{18}$$

According to the coefficients $x_2$, $x_1$, and $x_0$ obtained from the Eq.(18), the expression of the fitting polynomial $y(t)$ is as follows:

$$y(t) = x_0 + x_1 t + x_2 t^2 \tag{19}$$

The displacement $s(t)$ obtained after fitting is:

$$s(t) = \int v(t)dt - x_2 t^2 - x_1 t - x_0 \tag{20}$$

In addition, due to the loss of signal energy caused by polynomial fitting integration and die-trend term in time domain, the accuracy of traditional digital integration in time domain is reduced [24], so it is necessary to make up for the energy loss in the time domain integration process. According to the velocity signal energy $v_p$ and displacement signal energy $s_p$ calculated by Simpson integral rule, the energy loss $p_{v-s}$ in the process from velocity signal integration $v(t)$ to displacement signal $s(t)$ can be obtained as:

$$P_{v-s} = S_p - V_p = \sqrt{\sum_{t=0}^{N-1} s(t)^2} - \sqrt{\sum_{t=0}^{N-1} v(t)^2} \tag{21}$$

## IV. INTERGRAL ALGORITHM SIMULATION

In order to further illustrate the advantages and disadvantages of each integration algorithm, use sinusoidal signal and typical seismic recording signal EL-Centro-NS as input signals for simulation analysis, and the original input seismic wave is integrated based on the hybrid integration algorithm proposed in this paper, at the same time, it is converted into a motor control signal for earthquake simulation shaking table test.

### A. TIME DOMAIN AND FREQUENC DOMAIN INTEGRATION SIMULATION COMPARISON

Taking a piece of sinusoidal signal data as an example, according to the content of Section 1 in the article, perform time-domain integration and frequency-domain integration separately, and the results of the two kinds of integrals are shown in Figure.2 and Figure.3.

According to Figure.2 and Figure.3, for the original sine wave signal, the signal obtained by frequency domain integration is better than that obtained by time domain integration, the error caused by the second integration in the time domain is larger than the error generated by the first integration. The frequency domain characteristics of the two integrals are

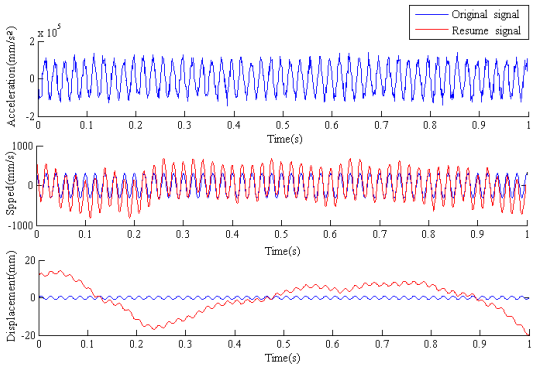


**FIGURE 2.** Acceleration integration result in time domain.

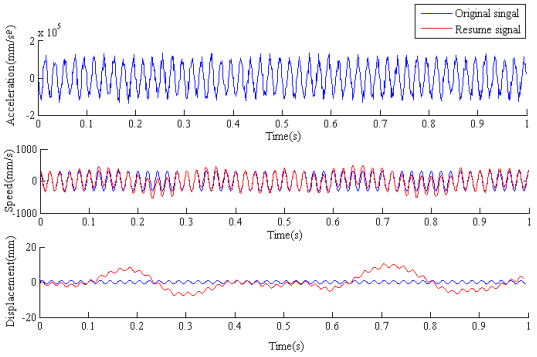


**FIGURE 3.** Acceleration integration results in frequency domain.

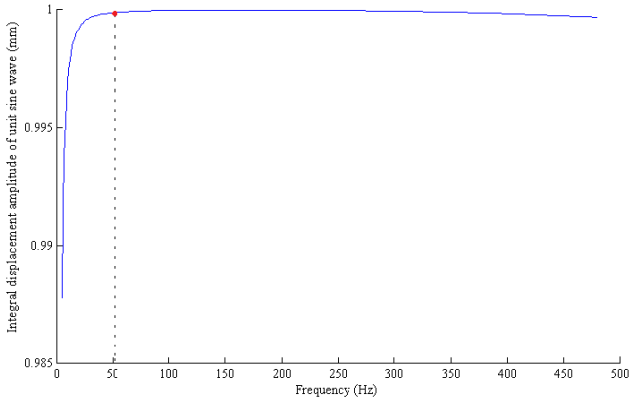


**FIGURE 4.** Frequency characteristic curve in time domain.

studied separately, the frequency characteristic curve in the time domain is shown in Figure.4, it can be found that the sinusoidal amplitude of the time domain integration recovered with the increase of the signal frequency will decrease, and the compliance of the low-band waveform is slightly worse than that of the high-band.

### *B. TIME SIMLATION ANALYSIS OF HYBRID INTERGRAL ALGORITHM*

Based on simulation studies in time and frequency domains, in order to study the improvement effect of the hybrid integration algorithm on the accuracy of seismic waveform reproduction, the acceleration input signal of the seismic wave simulation shaking table test is processed by the hybrid integration algorithm, and the motor control signal of the lower computer controller is obtained to complete the vibration test of the shaking table.

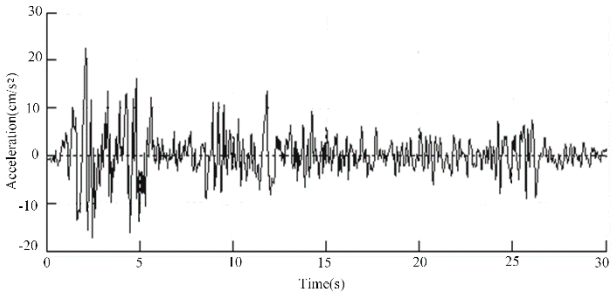


**FIGURE 5.** Seismic wave signal input.

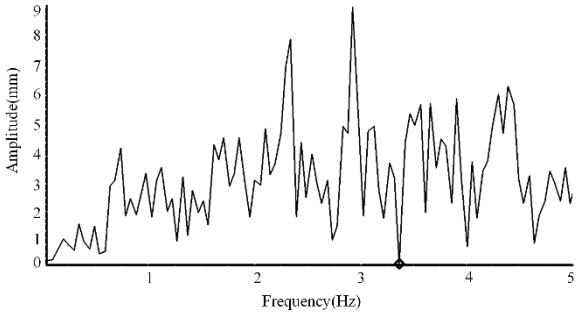


**FIGURE 6.** Acceleration Fourier amplitude spectrum.

With 220gal EL-Centro-NS as the input signal of seismic record signal, the input signal of seismic wave after 10 times scale of original seismic wave (as shown in Figure.5) and its corresponding Fourier amplitude spectrum of acceleration (as shown in Figure.6) can be obtained by MATLAB simulation, where the frequency corresponding to the first low point amplitude in the acceleration amplitude spectrum is 3.4 Hz. Since the acceleration low frequency signal has no obvious noise signal, Therefore, the low-frequency cutoff frequency and integration accuracy selected by the low-frequency attenuation algorithm in the frequency domain integration module of the hybrid integration algorithm are $f_T = 3.4\,\text{Hz}$ and $\partial_T = 0.98$.

According to the determined low-frequency cutoff frequency and integration accuracy, integrate the input acceleration signal (Figure.5) according to the process (Figure.1) to obtain the final displacement signal, and calculate the control signal required for each action of the servo motor. The resulting displacement signal is shown in Figure.7.

## V. HYBRID INTEGRAL SHAKING TABLE TEST

In order to verify the feasibility of the hybrid integral algorithm proposed, take the earthquake simulation shaking table of the Key Laboratory of Concrete and Prestressed Concrete Structure of the Ministry of Education of Southeast

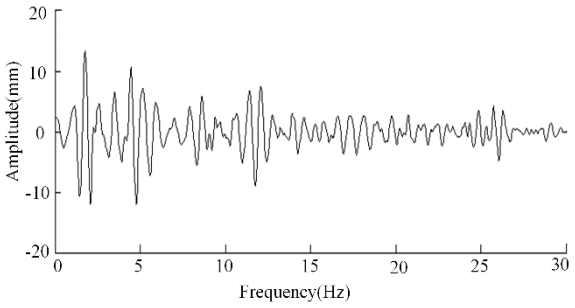


**FIGURE 7.** Displacement signal obtained after mixed integration.

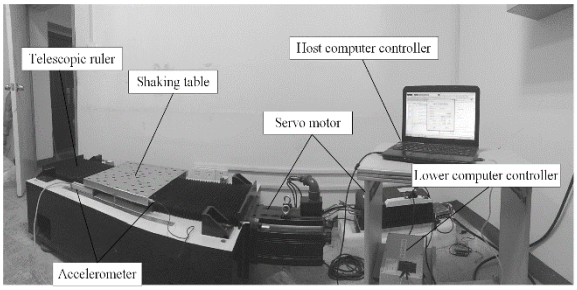


**FIGURE 8.** Earthquake simulation shaker.

University as the test object (Figure.8), the shaking table parameters are shown in Table 1. Inputting real seismic wave signal to the shaking table, and convert the data obtained based on the hybrid integration algorithm into the control data of the lower computer for shaking table test, the actual acceleration of the shaking table collected by the acceleration sensor is compared with the input acceleration to verify the seismic wave reproduction based on the hybrid integration algorithm, and analysis of the causes of errors.

### A. SERVO MOTOR CONTROL TEST

The vibration table control system selected in the test uses a servo motor as the excitation source of the system. The precise control of the servo motor is the guarantee of the normal operation of the system and an important part of ensuring the stable operation of the system. The control effect of the servo motor directly affects the accuracy of seismic wave reproduction. In this paper, the position/speed control mode of the servo motor is used, with position control as the main and speed control as the auxiliary to complete the control of the servo motor. In order to verify the control performance of the servo motor after adding speed control on the basis of position control, the following test is designed:

Sending a sinusoidal input motor control signal to the host controller of the lower computer, and use the displacement sensor to collect the position signal of the vibration table at every moment, the test result is shown in Figure.9. The test curve is basically consistent with the theoretical input curve, the test shows that after the speed control is added, the speed control results also meet the test requirements while maintaining the position control accuracy.

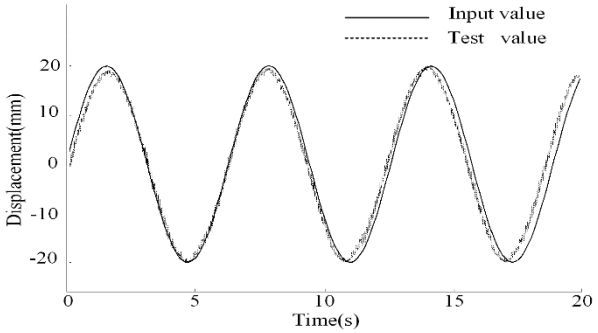


**FIGURE 9.** Sin wave input test.

**TABLE 1.** Dimensions of shaking table apparatus.

| name | size ( mm ) |
|---|---|
| Vibration table size | 500*500*40 |
| Vibration table base size | 1400*700*350 |
| Fixed block size | 120*80*80 |
| Screw diameter/pitch | 40/10 |
| Effective itinerary | 600 |

* **Effective itinerary**: the distance between the center point of the vibrating table base and the limit switches on both sides

### B. SEISMIC WAVE RECURRENCE TEST

Complete the verification of the effectiveness and feasibility of each key link of the shaker control system, and confirm the reliability of the shaker control system in the position/speed control mode from the perspective of the test. On this basis, the real seismic wave 220gal EL-Centro-NS is used as the input excitation of the vibration table, and a high-precision acceleration sensor is used to complete the collection of real-time acceleration data on the vibration table. In this test, the comparison between the acceleration time history of the vibration table and the EL-Centro-NS wave acceleration time history under the action of EL-Centro-NS wave is shown in Figure.10, it can be seen from Figure.10 (a), the peak acceleration of the input value is 220gal, which appears at 2.12s, and the peak acceleration of the test value is 211gal, which appears at 2.08s, the peak acceleration can basically be reproduced. The maximum error between the input value and the test value appears at 2.44s, and the value is 91gal; Figure.10 (b) is the partial magnification result of comparison of test acceleration time history, it can be clearly seen that the acceleration test values show good follow-ability during the test, and the acceleration reproduction results basically meet the requirements.

### C. ERROR EVALUATION INDEX AND TEST ERROR ANALYSIS

For quantitative analysis and evaluation of the accuracy of seismic wave repetition, according to the characteristics of the vibration signal, the average peak error *Erp* is introduced as the evaluation index of the accuracy of seismic wave

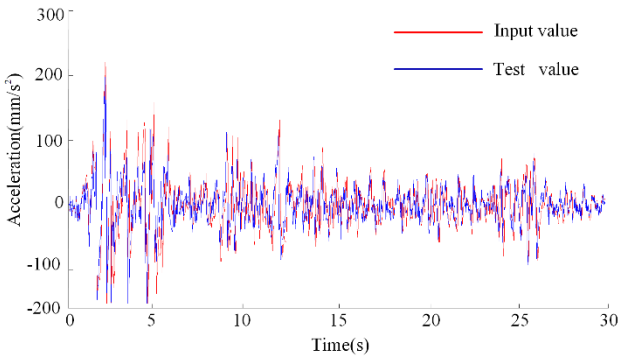


**(a) Acceleration time history comparison under EL Centro NS waver**

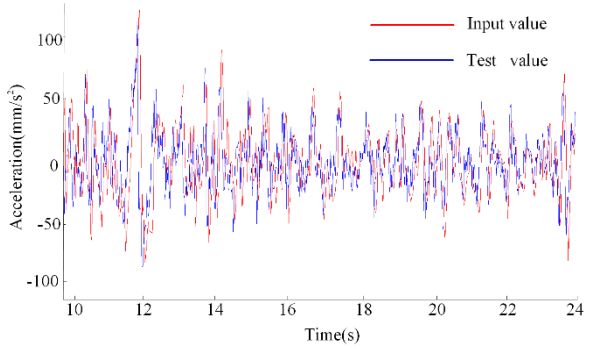


**(b) Local figure of acceleration time history comparison under EL Centro NS wave**

**FIGURE 10. Comparison of table acceleration input values and test results under EL Centro wave.**

repetition. The error calculation formula is:

$$Erp = \frac{1}{2}\left[\frac{\max X(t) - \max A(t)}{\max A(t)} + \frac{\min X(t) - \min A(t)}{\min A(t)}\right] \tag{22}$$

where: $X(t)$ is the original signal; $A(t)$ is the measured signal

The average peak error is the average value of the relative difference between the peak and valley of the input acceleration signal $x(t)$ relative to the actual measured acceleration $A(t)$, it mainly reflects the agreement between the original acceleration signal waveform and the maximum range of the measured acceleration waveform. Combining Eq. (22) and Figure 10, it can be seen that the maximum error at 2.44s is 49.8%, and the errors at other points are mostly controlled at around 10%. The test accuracy is greatly improved compared to the traditional seismic simulation shaker. For the error between the test value and the input value measured by the sensor during the test, the comprehensive analysis is mainly affected by the following factors:

(1) During the test, friction and other factors between the hardware structure connections will consume part of the energy.

(2) The maximum error points that exist in the process of waveform reproduction all occur after the maximum peak in the forward direction. This error is caused by the reverse acceleration that is not well reproduced when the vibration table overcomes the forward inertia. The number of error points is limited, so it will not have a large impact on the shaking table test results.

(3) Sensor error, the vibration table works in a lower frequency band, and most acceleration sensors have lower sensitivity under low frequency vibration conditions. At the same time, during data acquisition, environmental noise will affect the test data, so it will introduce Avoid interference.

(4) When the vibrating table is moving at a high speed, a large inertia will be generated, so that when the acceleration changes too much, the inertia will interfere with the control result.

## VI. CONCLUSION

Earthquake simulation shaking table is a scientific vibration test device that integrates the functions of structural excitation, performance testing and data analysis. It has a very important position in the seismic reduction and seismic research of building structures. In order to deal with the problem of poor accuracy of seismic waveform reproduction caused by large errors in the integration process of acceleration signals in the shaking table test of seismic simulation, a hybrid integration algorithm based on time-domain integration and frequency-domain integration is proposed to process the original acceleration signal of seismic waves, and a low-frequency attenuation algorithm and a polynomial fitting algorithm are fused to further reduce the integration error, through the integration simulation analysis and shaking table test to verify the performance of the hybrid integration algorithm.

Integration simulation and test results show that this method has obvious advantages over other integration methods in improving the accuracy of waveform reproduction in seismic simulation shake table tests. The two-time integration process reduces the cumulative effect of small errors in time-domain integration and the sensitive effects of low-frequency bands in frequency-domain integration, so that the waveform reproduction accuracy basically meets the requirements of shaker test, this algorithm has certain reference value for the shaker test research; because the seismic simulation shaker is a complex test device, therefore, the existence of systematic errors in the actual shaking table test is inevitable. Later, we will consider introducing an error compensation device during the shaking table test, and designing a test closed-loop structure to adjust the system error in real time, so that the seismic simulation shaking table has a higher waveform reproduction accuracy during the seismic waveform reproduction process.

## ACKNOWLEDGMENT

The author want to sincerely avail this opportunity to express my cordial thanks to those who have granted me invaluable instructions during the process of thesis writing.

## REFERENCES

[1] H. B. Liu and X. Guo, "Shaking table collapse comparison test analysis of typical masonry structure in polar earthquake area," *Chin. Civil Eng. J.*, vol. 12, no. 45, pp. 18–28, Dec. 2012.
[2] Z. B. Li and Z. Y. Tang, "Three parameters control algorithm for seismic simulation shake table overshoot correction," *Shock Vib.*, vol. 29, no. 10, pp. 211–215, Oct. 2010.
[3] F. W. Qiu and F. Q. Sha, "Research on the control technology and software of seismic simulation shaking table," *Hydraul. Pneumatic*, vol. 23, no. 6, pp. 98–101, Jun. 2011.
[4] L. K. Gao and Z. W. Chen, "Research on frequency division and recurrence method of seismic simulation test waveform," *Building Struct.*, vol. 48, no. S2, pp. 299–303, Dec. 2018.
[5] M. Z. Li, Z. Q. Wang, and Y. S. Liu, "Research on measurement method of micro displacement based on hybrid integration algorithm," *Instrum. Technique Sensor*, vol. 52, no. 12, pp. 118–122, Dec. 2017.
[6] S. A. Odhano, R. Bojoi, S. G. Rosu, and A. Tenconi, "Identification of the magnetic model of permanent-magnet synchronous machines using DC-biased low-frequency AC signal injection," *IEEE Trans. Ind. Appl.*, vol. 51, no. 4, pp. 3208–3215, Jul. 2015.
[7] U. Jon, J. Kim, and H. Lee, "DC motor current control algorithm using proportional-integral LQT with disturbance observer," *Int. J. Automot. Technol.*, vol. 19, no. 6, pp. 959–967, Dec. 2018.
[8] M. K. Gu and Z. H. Lv, "Discussion on the recognition method of vibration speed and displacement signal based on vibration acceleration measurement," *Mech. Sci. Technol.*, vol. 30, no. 4, pp. 522–526, Apr. 2011.
[9] Y. M. Hu, Y. J. Zhou, and H. Zhu, "Research and application of frequency domain integration algorithm based on trend term error control," *Shock Vib.*, vol. 34, no. 2, pp. 171–175, Jan. 2015.
[10] J. Wang and Z. Q. Wang, "Lagrange polynomial fitting method for numerical integration of the vibration acceleration," *Noise Vib. Control*, vol. 35, no. 6, pp. 191–196, Dec. 2015.
[11] B. Wu, T. L. Pan, and H. W. Yang, "Energy-consistent integration method and its application to hybrid testing," *Earthq. Eng. Struct. Dyn.*, vol. 49, no. 5, pp. 415–433, Feb.2020.
[12] W. Kim and S. Y. Choi, "An improved implicit time integration algorithm: The generalized composite time integration algorithm," *Comput. Struct.*, vol. 196, pp. 341–354, Feb. 2018.
[13] D. Krieg and E. Novak, "A universal algorithm for multivariate integration," *Found. Comput. Math.*, vol. 17, no. 4, pp. 895–916, Aug. 2017.
[14] Q. Zhang and X. Y. Zheng, "Walsh transform and empirical mode decomposition applied to reconstruction of velocity and displacement from seismic acceleration measurement," *Appl. Sci.*, vol. 10, no. 10, pp. 3508–3509, May 2020.
[15] Y. Zhu, W. L. Jiang, and X. D. Kong, "An accurate integral method for vibration signal based on feature information extraction," *Shock Vib.*, vol. 2015, no. 93, pp. 12–13, May 2015.
[16] M. Takiguchi, H. Sugimoto, N. Kurihara, and A. Chiba, "Acoustic noise and vibration reduction of SRM by elimination of third harmonic component in sum of radial forces," *IEEE Trans. Energy Convers.*, vol. 30, no. 3, pp. 883–891, Sep. 2015.
[17] Z. H. Xu and Q. Zhang, "Application of time domain integration in vibration signal analysis," *Vehicle Engine*, vol. 39, no. 4, pp. 87–92, Aug. 2016.
[18] M. Sun, Z. Li, Z. Li, Q. Li, Y. Liu, and J. Wang, "A noise attenuation method for weak seismic signals based on compressed sensing and CEEMD," *IEEE Access*, vol. 8, pp. 71951–71964, 2020.
[19] X. Cheng, T. Zhou, and K. Sun, "Research on vibration acceleration signal processing and time-frequency integration based on wavelet denouncing," *Power Energy*, vol. 40, no. 6, pp. 633–637, Dec. 2019.
[20] P. Sochala and F. De Martin, "Surrogate combining harmonic decomposition and polynomial chaos for seismic shear waves in uncertain media," *Comput. Geosci.*, vol. 22, no. 1, pp. 125–144, Feb. 2018.
[21] J. Breebaart, "Comparison of across-frequency integration strategies in a binaural detection model," *J. Acoust. Soc. Amer.*, vol. 134, no. 5, pp. EL407–EL412, Nov. 2013.
[22] P. Seiler, "Stability analysis with dissipation inequalities and integral quadratic constraints," *IEEE Trans. Autom. Control*, vol. 60, no. 6, pp. 1704–1709, Jun. 2015.
[23] Y. H. Hong, H. K. Kim, and H. S. Lee, "Reconstruction of dynamic displacement and velocity from measured accelerations using the variational statement of an inverse problem," *J. Sound Vib.*, vol. 329, no. 23, pp. 4980–5003, Nov. 2010.
[24] H. Zhou, "Research on the integration method of vibration acceleration signal in time and frequency domain," *Mech. Eng.*, vol. 50, no. 4, pp. 147–149, Apr. 2018.

**YING-QING GUO** received the Ph.D. degree in control theory and engineering from Southeast University, Nanjing, China, in 2010. From 2013 to 2019, she was an Associate Professor with the College of Mechanical and Electronic Engineering, Nanjing Forestry University, China, where she has been a Professor, since 2020. She is the author of two books, more than 50 articles, and more than 30 inventions. Her research interests include intelligent control, smart materials and structures, and vibration control.

**ZONG-YIN LI** is currently pursuing the M.A.Eng. degree in seismic simulation shaking table control technology with the College of Mechanical and Electronic Engineering, Nanjing Forestry University. His research interests include motor control, embedded systems, and intelligent control algorithms.

**XIAO-LU YANG** received the M.A.Eng. degree in control engineering from the College of Mechanical and Electronic Engineering, Nanjing Forestry University, China, in 2017. His current research interests include development of embedded system software and hardware and various development chips to independently complete the function construction of embedded systems.

**JIN-BAO LI** received the bachelor's degree in architectural engineering. He is a Senior Engineer with the Research Level and a National First-Class Registered Constructor. He is currently working with Jiangsu Southeast Special Engineering and Technology Company Ltd. He was engaged in design and construction of structural engineering construction and structural reinforcement for more than 40 years. He is responsible for 100's of cases of structural reinforcement design and construction of architectural engineering. He has presided over 12 of engineering projects with technological innovation and new technology application. He holds seven national invention patents and 17 national utility model patents. He has published more than 110 professional articles and coauthored four professional articles on structural reinforcement. His main research interests include building structure reinforcement technology, building displacement correction technology, deep foundation pit support technology, and building foundation reinforcement technology.